Available online at www.sciencedirect.com
SCIENCE DIRECT®
Journal of Magnetic Resonance 174 (2005) 254–264
JMR Journal of Magnetic Resonance
www.elsevier.com/locate/jmr

Theoretical and experimental investigation of ^{13}C relayed ^{2}H–^{2}H-COSY 2D experiments: Application to the analysis of weakly aligned solutes

Olivier Lafon, Philippe Lesot *

Laboratoire de Chimie Structurale Organique, CNRS UMR 8074, ICMMO, Bât. 410, Université de Paris-Sud, 91405 Orsay, France

Received 8 December 2004; revised 8 December 2004
Available online 12 March 2005

Abstract

We describe new NMR 2D experiments denoted DECADENCY for DEuterium CArbon DEuterium Nuclear Correlation spectroscopY dedicated to the analysis of anisotropic deuterium spectra. They belong to the class of X-relayed Y,Y-COSY 2D experiments that was initially explored in the case of a ^{1}H–X–^{1}H fragment ($I_X = 1/2$) in isotropic medium. DECADENCY 2D experiments permit to correlate the quadrupolar doublets associated with two inequivalent deuterium nuclei in an oriented CD_2 fragment through heteronuclear polarization transfers. Two kinds of pulse sequences are described here using either a double INEPT-type or DEPT-type process. DECADENCY 2D experiments provide an interesting alternative to ^{2}H–^{2}H COSY experiments when the geminal ^{2}H–^{2}H total coupling (scalar and dipolar) is null or too small to provide visible cross-correlation peaks. Such a situation is typically observed for geminal deuteriums in prochiral or chiral molecules dissolved in chiral liquid crystals. The efficiency of these techniques is illustrated using dideuterated prochiral molecules, the phenyl[$^{2}H_2$]methanol and the 1-chloro[1-$^{2}H_2$]nonane, both dissolved in organic solutions of poly-γ-benzyl-L-glutamate. The advantages of each sequence are presented and discussed. It is shown that the relative sign of the quadrupolar doublets can be determined.

Keywords: ^{2}H NMR spectroscopy; Quadrupolar splittings; Chiral liquid crystals; C–D polarization transfers

1. Introduction

NMR spectroscopy in chiral polypeptide oriented solvents is now a well-established technique [1–4]. It provides efficient and original solutions to organic chemists for investigating enantiomeric purity of a mixture, analyzing stereochemistry or answering to a specific analytical problem.

As a typical example, we have recently studied the mechanism of SmI_2 mediated cyclization of δ-iodo-α, β-unsaturated esters using proton-decoupled deuterium NMR (^{2}H–{^{1}H}) in PBLG solvents as spectral tool [5]. Actually in the course of this work, we have developed an interesting strategy for distinguishing *meso* from *d*,*l* stereoisomers in a mixture, and then for safely assessing diastereoisomeric and enantiomeric purity. In a first step, a "CD_2" probe was introduced in the molecules under studied, thus leading to a 1D ^{2}H–{^{1}H} spectrum made of six resolved quadrupolar doublets centered approximately on the same chemical shift, two associated with the *meso* compound, four associated with the enantiomers. In a second step, proton-decoupled deuterium COSY 2D experiments in chiral and achiral anisotropic phases were performed and allowed to pair up and assign quadrupolar doublets belonging to *meso* and *d*,*l* stereoisomers on the basis of ^{2}H–^{2}H correlation peaks in the 2D map [5].

* Corresponding author. Fax: +33 01 69 15 81 05.
E-mail address: philesot@icmo.u-psud.fr (P. Lesot).

1090-7807/$ - see front matter © 2005 Elsevier Inc. All rights reserved.
doi:10.1016/j.jmr.2005.02.011

It can be argued here that deuterium–carbon correlation experiments could be used for pairing up the quadrupolar doublets of *meso* and *d*,*l* isomers [6,7]. This solution is pertinent but was not applicable because the difference of carbon-13 chemical shifts for the carbon atom in the CD_2 probe in the *meso* and *d*,*l* isomers was too small to provide separated resonances (at least at 9.4 T).

In this approach, the pairing up and subsequently the assignment of doublets using COSY 2D experiments is only possible when the ^2H–^2H total coupling (scalar and dipolar) between geminal deuterium nuclei is sufficiently large in magnitude to produce cross-correlation peaks visible on the 2D map. As organic solutions of polypeptide orient any solutes rather weakly, this condition could be not always fulfilled.

A priori, such a problem should not exist anymore if we are able to correlate deuterium nuclei in the CD_2 probe, transferring the polarization stepwise from ^2H to ^{13}C and back to ^2H. In this scheme, cross-correlations should be governed by one-bond carbon–deuterium total couplings, $^1T_{CD}$ with $^1T_{CD} = {}^1J_{CD} + 2\ {}^1D_{CD}$. Disregarding the spurious cases where $^1T_{CD}$ is small ($^1J_{CD} \approx -2\ {}^1D_{CD}$) or null ($^1J_{CD} = -2\ {}^1D_{CD}$), the magnitude of $^1T_{CD}$ is generally distributed around the value of scalar couplings $^1J_{CD}$, namely about 20–30 Hz. Consequently, cross-correlations between geminal deuterons should be always detected whatever the magnitude of the homonuclear ^2H–^2H couplings.

In the first part of this work, we theoretically describe new 2D experiments, called DECADENCY (DEuterium CArbon DEuterium Nuclear Correlation spectroscopY), that allow the correlation between the quadrupolar doublets of inequivalent deuterons bonded to the same carbon-13 atom without the need of ^2H–^2H dipolar couplings. Two pulse sequences using two consecutive polarization transfers (PT) are proposed. They use either an INEPT-type or a DEPT-type transfer mechanism. In the second part, the efficiency of these sequences is studied using prochiral molecules of C_s symmetry: the phenyl[$^2H_2$]methanol and an equimolar mixture of this molecule and 1-chloro[1-$^2H_2$]nonane. Both samples are dissolved in an oriented organic solution of poly-γ-benzyl-L-glutamate (PBLG) in chloroform. The experimental results obtained using both 2D sequences are reported and discussed.

2. Theoretical analysis

DECADENCY 2D experiments are homonuclear experiments based on a relayed heteronuclear transfer mechanism. They belongs to the class of X-relayed Y,Y-COSY 2D experiments that was pioneered by Lallemand and next by Wüthrich in the case of a ^1H–X–^1H fragment [8,9]. To the best of our knowledge, such a concept was only applied to spin-1/2 nuclei in isotropic phase, and was never explored in case of a D-X-D fragment ($I_X = 1/2$) aligned in a liquid crystal, so far. The main difference between a ^1H–X–^1H and ^2H–X–^2H fragment arises from the presence of the quadrupolar interaction associated with spin-1 nuclei in oriented solvent.

After a double Fourier transformation, the 2D map of DECADENCY experiments must be formally equivalent to the ^2H–^2H COSY 2D map. It contains the same kind of spectral information [5], namely diagonal peaks (DP), autocorrelation peaks (AP), and cross-correlation peaks (CP) for a $^{13}CD_2$ spin (see Fig. 2A). However in DECADENCY experiments, all signals result from two consecutive PT's via the one-bond ^{13}C–^2H total couplings. In this scheme, CP's correspond to the case where polarization is transferred from deuterium to carbon-13 nucleus, and then transferred back to the second deuterium ($D^i \rightarrow {}^{13}C \rightarrow D^j$) in a CD_2 group. On the other hand, DP's and AP's correspond to the case where polarization is transferred from deuterium to carbon-13 nucleus and then returns to the same deuterium ($D^i \rightarrow {}^{13}C \rightarrow D^i$). In this aim, two mechanisms of C–D polarization transfers involving either a double INEPT-type or a DEPT-type process can be considered [10–12]. Both of schemes present advantages and limits, and hence they will be examined below.

To determine analytical expressions for the different signals in the DECADENCY 2D experiments, we used the product-operator formalism developed for two non-equivalent deuterium nuclei denoted D^i and D^j, coupled to the same carbon via $^1T_{CD}$. For our purpose, we have considered the simplest relevant case where the geminal ^2H–^2H coupling is disregarded. A brief description of various product operators associated to this system and their evolution under the influence of ^{13}C–^2H coupling are given in Appendix A. In according with previously reported approaches for spin-1/2 [13,14], the evolution of product operators during the sequences was calculated with *Mathematica* [15]. As a result of the large number of terms involved, only the evolutions contributing to the final signal are considered. Note also that the geminal deuterium nuclei, D^i and D^j, behave identically and have an interchangeable role. Consequently for the clarity, the spin labels 'i,j' and 'j,i' used in the product operators or in equations, mean 'i or j' and 'j or i', respectively. The superscript notation 'C' will be relative to the carbon-13 nucleus.

2.1. Double INEPT polarization transfer

The standard DECADENCY sequence based on two consecutive INEPT-type polarization transfers, simply derives from the well-known HETCOR pulse sequence that was recently used to correlate deuterium to carbon in weakly orienting media (CDCOM 2D experiment)

[6,7]. Actually, compared against the CDCOM experiment, a further INEPT transfer of polarization from the carbon-13 to deuterium nucleus is introduced just before the acquisition period of signal. The pulse scheme of the sequence (denoted DECADENCY-INEPT) is given in Fig. 1A. During the variable evolution period t_1, deuterium single quantum coherences evolve under the influence of chemical shift and quadrupolar interaction, while the ^{13}C–^{2}H total couplings, T_{CD}, are refocussed by the ^{13}C π pulse at the midpoint of t_1.

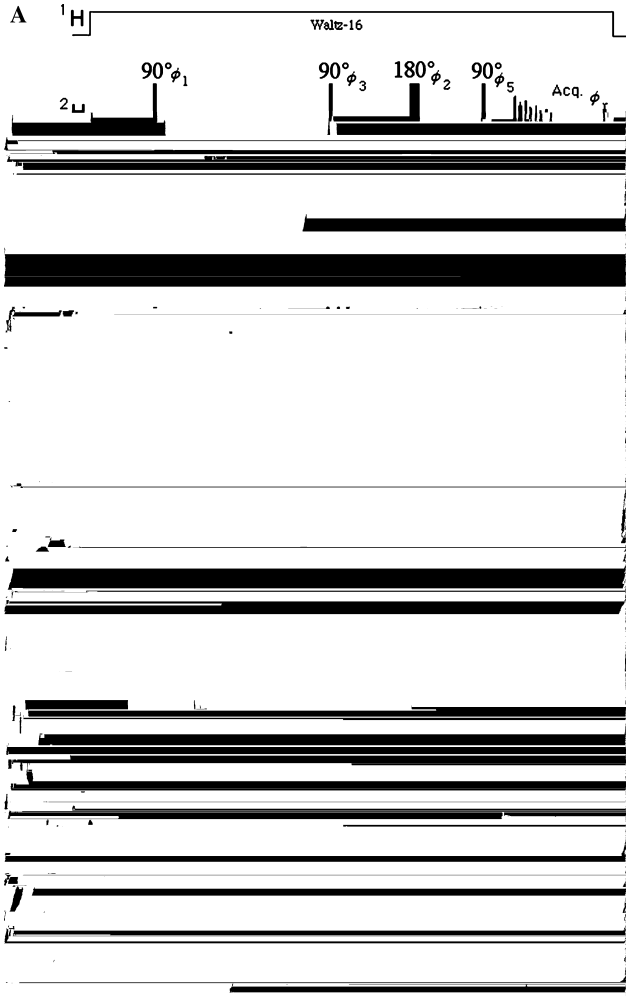

Fig. 1. Pulse scheme and coherence transfer pathway diagram for correlation peaks in DECADENCY experiments based on either two consecutive INEPT-type PTs (A and B) or DEPT-type PTs (C and D). The basic 4-step phase cycling is: $\phi_1 = 2(x), 2(-x)$; $\phi_2 = \phi_3 = \phi_5 = \phi_6 = 4(x)$; $\phi_4 = 2(x,-x)$; $\phi_r = x,-x,-x,x$ and $\phi_1 = 2(x), 2(-x)$; $\phi_2 = \phi_4 = \phi_5 = 4(x)$; $\phi_3 = 2(x,-x)$; $\phi_r = x,-x,-x,x$, respectively. Quadrature detection in F_1 dimension uses TPPI method ($\pi/2$ phase increment of the first pulse). The choice of values for the τ and τ' delays is discussed in the text. In both experiments, the proton nuclei are decoupled by applying the Waltz-16 sequence whilst the Garp-4 sequence suppresses ^{13}C–D couplings during the aquisition period. A 180° composite pulse in the middle of t_1 can be implemented to improve the refocussing of ^{13}C–D couplings.

The removal of heteronuclear couplings by refocussing has the advantage of requiring much less average power than broadband decoupling. The C–D coupling evolves during the first delay τ, leading to an antiphase magnetization of deuterium with respect to ^{13}C–^{2}H coupling, and corresponding to the product operator $2I_x^{i,j}S_z^C E^{j,i}$. In the following, the identity operator, E, will be omitted. Deuterium coherences are then converted into ^{13}C coherences during the first step of polarization transfer ($D^{i,j} \rightarrow {}^{13}C$) that is made by the simultaneous application of ^{2}H and ^{13}C $\pi/2$ pulses.

At this step of the sequence and after four-step phase cycle, the density operator contains the terms: $2I_z^{i,j}S_y^C$, $2I_x^{i,j}S_y^C$, $2K_y^{i,j}S_y^C$, and $2D_y^{i,j}S_y^C$. The term, $2I_z^{i,j}S_y^C$, is representative of antiphase y-magnetization of ^{13}C with respect to ^{13}C–^{2}H coupling. The second and third term, $2I_x^{i,j}S_y^C$ and $2K_y^{i,j}S_y^C$, correspond to the ^{13}C–^{2}H heteronuclear zero- and double-quantum coherence, in-phase and antiphase, respectively, with respect to quadrupolar doublet. Finally, the fourth one, $2D_y^{i,j}S_y^C$, corresponds to the ^{13}C–^{2}H heteronuclear single- and triple-quantum coherence. Note that the terms, $2I_z^{i,j}S_y^C$ and $2I_x^{i,j}S_y^C$, are "formally analogous" to that obtain in the case of a PT between two spin-1/2 nuclei while $2K_y^{i,j}S_y^C$ and $2D_y^{i,j}S_y^C$ are specific of the polarization transfer from spin-1 to spin-1/2 nucleus [10]. However, the final evolution of the four previous operators indicates that the antiphase ^{13}C magnetization (associated to a single coherence) contributes to the signal of CP's, DP's, and AP's, while the other terms contribute to DP's and AP's only. Note here that the two first steps of the phase cycle restrict the observed signal during t_2 to the terms directly deriving from the four previous product operators, thus eliminating the undesired signals of deuterium nuclei bound to ^{12}C. The remaining two steps remove axial peaks arising from pure longitudinal ^{13}C magnetization during t_1. A more sophisticated phase cycle or pulse field gradients could be proposed to strictly select ^{13}C 1Q-coherence, $2I_z^{i,j}S_y^C$, during τ' period. Nevertheless the use of pulse field gradients produce loss of sensitivity, while the increase of step number in phase cycle can generate unuseful artifacts [16]. On the other hand, the presence of $2D_y^{i,j}S_y^C$ term is not cumbersome while heteronuclear two-spin zero- and double-quantum coherences also contribute (weakly) to the signal of CP's when the deuterium–deuterium coupling is not null.

In DECADENCY 2D experiments, only cross-correlation peaks provide the relevant information, consequently we focus our attention on the evolution of the antiphase ^{13}C magnetization. During the τ' period, only ^{13}C chemical shifts are refocused by applying two simultaneous ^{2}H and ^{13}C π pulses at the middle point. The antiphase ^{13}C magnetization is then converted into antiphase ^{2}H magnetization with respect to ^{13}C–^{2}H coupling ($C \rightarrow D^{j,i}$) by applying again two simultaneous ^{2}H and ^{13}C $\pi/2$ pulses. At this step of the sequence, the deute-

rium magnetization contains the terms $2I_y^{i,j}S_z$, $I_y^{i,j}S_z^C Q_z^{j,i}$, $2S_z^C I_y^{j,i}$, and $Q_z^{i,j}S_z^C I_y^{j,i}$. Among these four product operators, only the first and third operator products will give rise to observable signals during t_2 if $^2T_{DD}$ is null. If the first term finally contributes to signal of DP's and AP's, the third one contributes to the CP signals. During the second delay τ, the evolution of antiphase ^{2}H magnetization under the influence of $^1T_{CD}$ coupling leads to an in-phase ^{2}H magnetization with respect to ^{13}C–^{2}H coupling, which is observable during acquisition when the broad-band carbon decoupling sequence is turned on. Finally, after a four-step phase cycle and disregarding all relaxation terms and phase factors, the expression of cross-correlation signals is:

$$S_{CP}(t_1,t_2) \propto \frac{2}{3}\mathrm{i}\{\sin[\omega_{D^{i,j}}(t_1+\tau)]\cos\lfloor\omega_{Q^{i,j}}(t_1+\tau)\rfloor\} \times \left\{\begin{array}{l}\sin[\omega_{CD^{i,j}}(\tau)]\sin[2\omega_{CD^{i,j}}(\tau')] \\ \times \sin[2\omega_{CD^{i,j}}(\tau')]\sin[\omega_{CD^{i,i}}(\tau)]\end{array}\right\} \times \left\{\begin{array}{l}e^{i[\omega_{D^{j,i}}(\tau+t_2)]-\omega_{Q^{j,i}}(\tau+t_2)]} \\ +e^{i[\omega_{D^{j,i}}(\tau+t_2)]+\omega_{Q^{j,i}}(\tau+t_2)]}\end{array}\right\}. \quad (1)$$

In this equation $\omega_D = 2\pi\nu_D$, $\omega_Q = \pi\Delta\nu_Q$ and $\omega_{CD} = \pi\,{}^1T_{CD}$, where $^1T_{CD}$ is the one-bond ^{13}C–^{2}H total coupling. The position of terms in the equation allows a better presentation of the evolution of signal during the periods t_1, τ, τ', and t_2.

After a four-step phase cycle and disregarding all relaxation terms and phase factors, the expression of diagonal and autocorrelation signals following the same coherence order (1Q) than for cross-correlation signals during τ' is:

$$S_{DP\ and\ AP}(t_1,t_2) \propto \frac{1}{3}\mathrm{i}\{\sin[\omega_{D^{i,j}}(t_1+\tau)]\cos[\omega_{Q^{i,j}}(t_1+\tau)]\} \times \left\{\begin{array}{l}\sin^2[\omega_{CD^{i,j}}(\tau)]\cos[2\omega_{CD^{i,j}}(\tau')] \\ \times(1+2\cos[2\omega_{CD^{i,i}}(\tau')])\end{array}\right\} \times \left\{\begin{array}{l}e^{i[\omega_{D^{i,j}}(\tau+t_2)-\omega_{Q^{i,j}}(\tau+t_2)]} \\ +e^{i[\omega_{D^{i,j}}(\tau+t_2)+\omega_{Q^{i,j}}(\tau+t_2)]}\end{array}\right\}. \quad (2)$$

As it can be seen from the Eqs. (1) and (2), the efficiency of the two consecutive PTs strongly depends on the value of τ and τ' delays. Disregarding relaxation effects, the intensity of CP's (I_{CP}) varies with τ as $\sin[\omega_{CD^{i,j}}(\tau)]\sin[\omega_{CD^{j,i}}(\tau)]$ while intensities of DP's and AP's (I_{DP} and I_{AP}) vary as $\sin^2[\omega_{CD^{i,j}}(\tau)]$ (the chemical shift and the quadrupolar interaction only modulate the peak phase). In the ideal case, where $^1T_{CD^i} = {}^1T_{CD^j} = T_{CD}$, I_{DP}, I_{AP}, and I_{CP} would be maximized when $\tau = 1/(2|T_{CD}|)$. With regard to the dependence with τ' (disregarding relaxation terms), the intensity of CP's is modulated as $\sin[2\omega_{CD^{i,j}}(\tau')]\sin[2\omega_{CD^{j,i}}(\tau')]$ while intensities of DP's and AP's are modulated as $(1+2\cos[2\omega_{CD^{i,i}}(\tau')])$. Here again, the choice of τ' affects the relative intensity of AP's and DP's compared to CP's. Thus, in the ideal case where $^1T_{CD^1} = {}^1T_{CD^2} = T_{CD}$, we can demonstrate that I_{CP} is maximum (I_{CPmax}) when $\tau' = 1/(4|T_{CD}|)$. In contrast when $\tau' = 1/(3|T_{CD}|)$, I_{DP} and I_{AP} are equal to zero and $I_{CP} = 3/4(I_{CPmax})$. This case is simulated in Fig. 2B. Finally, when $\tau' = 1/(2|T_{CD}|)$, $I_{CP} = 0$, and only the DP's and AP's are observed in the 2D spectrum. Actually, when $\Delta\nu_{Q^1} \neq \Delta\nu_{Q^2}$, the ideal case where $^1T_{CD^1} = {}^1T_{CD^2}$ does not exist, and hence in practice, DP's, AP's, and CP's are never totally suppressed as expected theoretically.

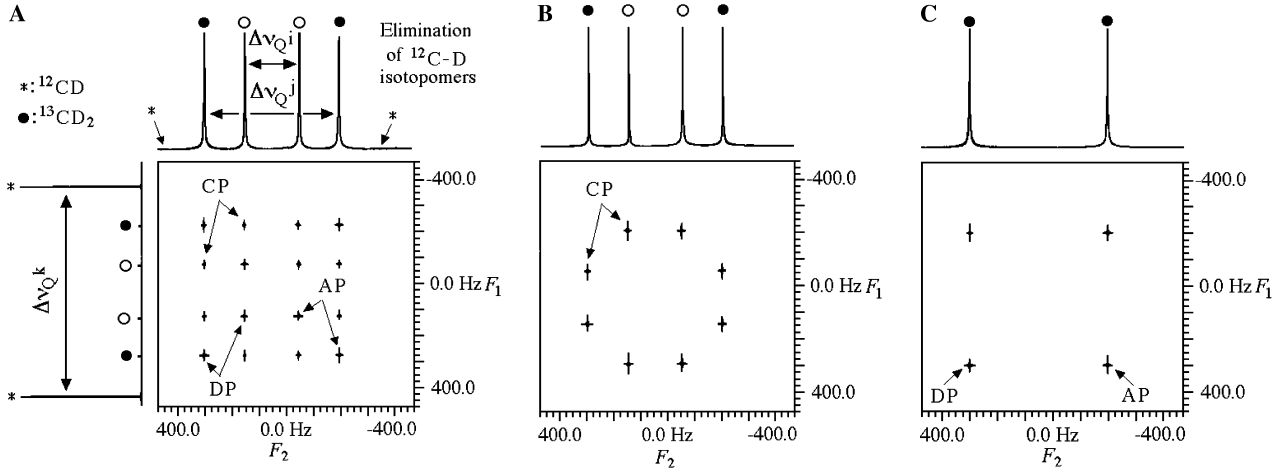

Fig. 2. Numerical simulations of the DECADENCY-INEPT 2D experiment (magnitude mode) on a fictitious ^{12}CD (98.9%) spin system and $^{13}CD_2$ spin system (1.1%) with two non-equivalent deuterium nuclei ($\delta_{D^i} = \delta_{D^j} = \delta_{D^k} = 1$ ppm, $\Delta\nu_{Q^i} = 200$ Hz, $\Delta\nu_{Q^j} = 500$ Hz, and $\Delta\nu_{Q^k} = 800$ Hz) in $^2T_{D^iD^j}$ is assumed to be zero. In the simulations (A and B), $^1T_{CD^i} = {}^1T_{CD^j} = 30$ Hz (ideal case but non realistic if $\Delta\nu_{Q^i} \neq \Delta\nu_{Q^j}$) and (C) $^1T_{CD^i} = 0$, $^1T_{CD^j} = 30$ Hz. The delay τ is set to 16.7 ms ($1/[2T_{CD}]$) whereas the delay τ' is equal to 8.3 ms ($1/[4T_{CD}]$) for simulation (A and C) and 11.1 ms ($1/[3T_{CD}]$) for (B). In F_1 dimension of the contour plot (A), the 1D spectrum showing the signal of ^{12}CD and $^{13}CD_2$ spin system is displayed. In F_2 dimension is given the projection of the 2D map. Note the elimination of undesired signals of deuteriums bound to ^{12}C by the phase cycling. The diagonal, autocorrelation and cross-correlation peaks are denoted DP, AP, and CP. On the third simulation (C), only the DP's and AP's associated with deuterium j are visible ($^1T_{CD^j} \neq 0$).

As a result of the low dispersion of $^1T_{CD}$'s for weakly aligned solutes, the average of $^1T_{CD}$'s gives in general good results, but this point will be examined further during the discussion of experimental results.

From Eqs. (1) and (2), it clearly appears that CP's disappear if one of the two $^1T_{CD}$s is equal to zero. This particular spectral situation is illustrated in Fig. 2C. In this last example, only DP's and AP's associated with the quadrupolar doublet of the deuterium (here D^j) sharing a non-zero coupling with the carbon-13 atom ($^1T_{CD^j} \neq 0$) is visible on the 2D map. These peaks originate from a double C–D polarization transfer involving the same deuterium, namely $D^{i,j} \rightarrow {}^{13}C \rightarrow D^{i,j}$.

2.2. Double DEPT polarization transfer

An alternative to the C–D INEPT-type PT is provided by the C–D DEPT-type PT that involved heteronuclear multiple-quantum (0 and 2) coherences [17]. This type of transfer can be implemented in the DECADENCY 2D experiment. The pulse scheme and the coherence transfer pathway diagram for cross-correlation signals of this second experiment (denoted DECADENCY-DEPT) are given in Figs. 1C and D. The pulse block yielding two consecutive PT's is simpler compared to the previous one. It is only made of two single carbon-13 $\pi/2$ pulses separated by two simultaneous deuterium $\pi/2$ pulses and carbon-13 π pulse at the midpoint of the refocussing delay τ'. Note that phase cycle of DECADENCY-INEPT and DECADENCY-DEPT experiments removes the same coherence transfer pathways.

Compared with the DECADENCY-INEPT sequence, the time evolution of the density operator of the DECADENCY-DEPT sequence is identical up to the first carbon-13 $\pi/2$ pulse. This last pulse converts antiphase ^2H magnetization with respect to ^2H–^{13}C coupling into heteronuclear zero- and double-quantum coherences. After a four-step phase cycle, the density operator at the beginning of the τ' period contains the terms, $2I_x^{i,j}S_y^C$, $2I_y^{i,j}S_y^C$, $2K_x^{i,j}S_y^C$, and $2K_y^{i,j}S_y^C$, that are associated to the ^{13}C–^2H heteronuclear zero- and double-quantum coherences (see Appendix A). Contrarily to the DECADENCY-INEPT 2D sequence, these four product operators evolving during τ' finally lead to CP's as shown in the coherence pathway diagram. Actually, in this scheme, the coherence pathways contributing to signal of DP's and AP's are the same than for CP's. During the interval τ', the coherences evolve under the influence of the ^{13}C–^2H coupling, the ^2H chemical shifts and ^2H quadrupolar interactions while ^{13}C chemical shift is refocused by the ^{13}C π pulse. The ^2H $\pi/2$ pulse at the midpoint of τ' permits to transfer heteronuclear coherences from one geminal deuterium nucleus toward the other one. The last ^{13}C $\pi/2$ pulse converts heteronuclear multi-quantum coherences into detectable ^2H magnetization. After a four-step phase cycle and disregarding all relaxation terms and phase factors, the expression of CP's is:

$$S_{CP}(t_1,t_2) \propto -\frac{1}{3} \sin[\omega_{CD^{i,j}}(\tau)] \sin[2\omega_{CD^{i,j}}(\tau'/2)] \times \sin[2\omega_{CD}6.7148665212(2)Tjj\ CD \times i[(\omega_{D^{i,j}}+\omega_{Q^{i,j}})(\tau'/2+\tau+t')]$$

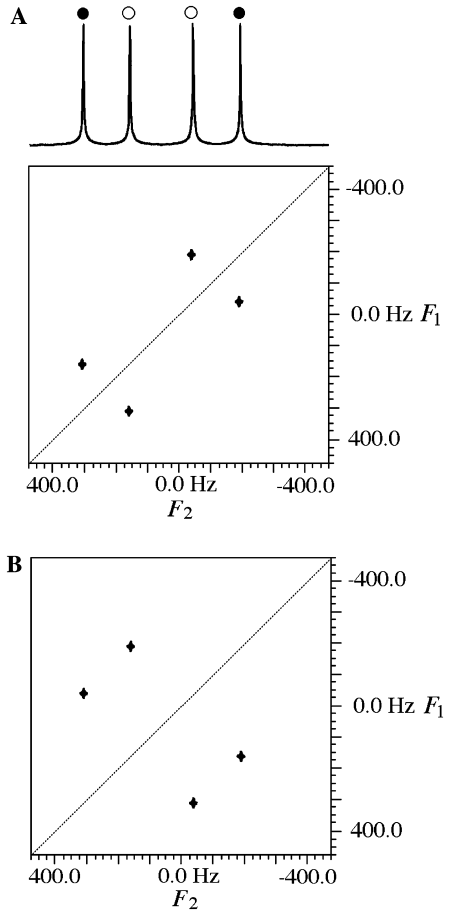

Fig. 3. Numerical simulation (magnitude mode) of the DECADENCY 2D experiment using a double DEPT-type transfer on a fictitious $^{13}CD_2$ spin system with two non-equivalent deuteriums (apart from the sign of quadrupolar splittings, the spin-system parameters are identical to those given in caption of Fig. 2) in an oriented medium. In both experiments, the delays τ are τ' are set to $1/(2|T_{CD}|)$. The signs of quadrupolar splittings are identical (positive or negative) in the simulation (A) and opposite in the simulation (B). Note the change of localization of CP's on the 2D map.

on the 2D map depends on the relative sign of quadrupolar doublets. In contrast, the position of CP's is independent on the sign of $^1T_{CD}$'s. As illustration, Fig. 3B presents an example of simulated 2D map where the CP's are distributed perpendicularly to the main diagonal, corresponding to the case where the signs of quadrupolar splittings are opposite.

3. Experimental section

3.1. Sample preparation

The NMR sample of phenyl[$^2H_2$]methanol (**1**) was prepared using 50 mg solute, 100 mg PBLG with a DP = 562, MW ≈ 120,000, (purchased from Sigma), and 350 mg of dry chloroform. The NMR sample of equimolar mixture of **1** and 1-chloro[1-$^2H_2$]nonane (**2**) was made by adding 76.7 and 50.1 mg of these solutes dissolved in 100 mg PBLG and 350 mg chloroform. The components of the mixture were weighed into a 5 mm o.d. NMR tube which was sealed to avoid solvent evaporation. Other experimental details can be found in [3].

3.2. NMR spectroscopy

The 2D experiments were performed at 9.4 T on a Bruker DRX 400 high-resolution spectrometer equipped with a 5 mm four-channel probe (QXO) operating at 61.4 MHz for deuterium and 100.6 MHz for carbon. This probe allows the matching and tuning of deuterium channel (outer coil), but the deuterium channel (lock) of any probes (dual or broadband) can be used to perform such experiments. The temperature of the sample was maintained at 300 K by the standard variable temperature unit of spectrometer (BVT 3200) and the experiments were performed without sample spinning. All 2D matrices were zero-filled to 1k (t_1) × 2k (t_2) data points prior to the double Fourier transformation. Unless otherwise specified, 2D contour plots are displayed in magnitude mode. Other experimental NMR parameters or details are given in the figure captions.

4. Results and discussion

To experimentally explore and illustrate the potentialities of the DECADENCY 2D experiments, we investigate the case of **1** dissolved in the PBLG/$CHCl_3$ phase at 300 K. In a chiral oriented medium, the C–D enantiotopic directions of this prochiral molecule of C_s symmetry in average are non-equivalent and exhibit two quadrupolar doublets (and distinct C–D total couplings) corresponding to the *pro-R and pro-S* deuterium atoms [18]. As it is not possible to assign these splittings by NMR spectroscopy, the labels A and B are used. In this example, the splittings measured for D^A and D^B are equal to $|\Delta\nu_{Q^A}| = 215$ Hz and $|\Delta\nu_{Q^B}| = 330$ Hz. The exact values of $|^1T_{CD}|$'s determined from the analysis of ^{13}C–{^1H} 1D spectrum are 27 and 31 Hz.

Fig. 4A presents the DECADENCY-INEPT 2D map of **1** displayed at low contour plot level when $\tau = 1/(2T_{CD})$ and $\tau' = 1/(4T_{CD})$ with T_{CD} set to the average value of $|^1T_{CD}|$'s, i.e., 29 Hz. As expected, 16 peaks (4 × 4) corresponding to the various types of peaks generated by the sequence are observed. The presence of CP's allows the correlation between geminal deuterium nuclei D^A and D^B bonded to the prostereogenic carbon of the molecule. Contrarily to the simulations, the intensities of four DP's and AP's are not equal. Disregarding effects due to pulse imperfections (that can be reduced by using composite pulses), this situation arises because experimentally $^1T_{CD^i} \neq {}^1T_{CD^j}$. If the average value of $|^1T_{CD}|$'s provides a suitable compromise for calculating the τ

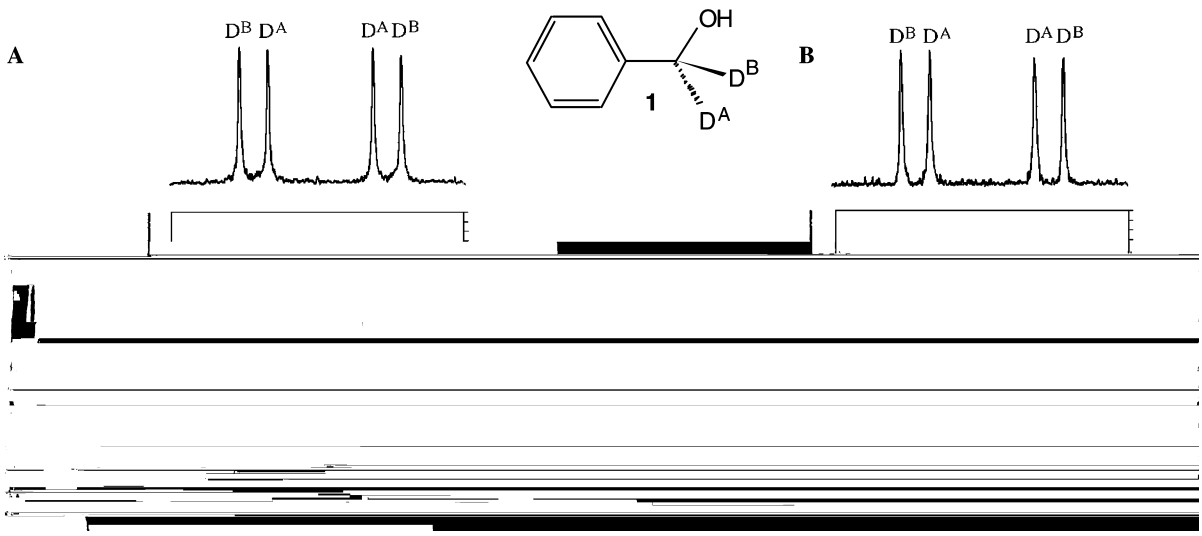

Fig. 4. DECADENCY-INEPT 2D spectra of **1** obtained when (A) $\tau = 1/(2T_{CD})$, $\tau' = 1/(4T_{CD})$ and (B) $\tau = 1/(2T_{CD})$, $\tau' = 1/(3T_{CD})$ with $T_{CD} = 29$ Hz. Both spectra have been recorded in the same conditions, using 128 (t_1) × 478 (t_2) data points and 320 scans per t_1 increment. No filtering and no symmetrization were applied here. In F_1 dimension is displayed the ^2H–{^1H} 1D spectrum of **1** while in F_2 dimension is given the projection of the 2D map. The assignment of quadrupolar splittings (A and B) relative to the molecular numbering is arbitrary.

delay, the difference between the ideal and the set value generates variations in peak intensity. This effect is, however, not really cumbersome for analyzing of the 2D map.

Fig. 4B shows the DECADENCY-INEPT 2D experiment of **1** when $\tau = 1/(2T_{CD})$ and $\tau' = 1/(3T_{CD})$. On the 2D map plotted and with high level contour plot, only CP's are visible, but DP's and AP's are not totally suppressed as expected by theory and they can be seen at lower contour plot levels. The reasons given previously explain also the origin of the presence of residual DP's and AP's in the 2D map. The same phenomenon was observed for the DECADENCY-DEPT 2D experiments.

Actually, another phenomenon involving ^2H–^2H couplings participates to the intensity variations observed on the 2D maps. To simplify the theoretical part, we have disregarded the contribution of the homonuclear couplings to the signal, but the experimental situation is more complex. Indeed if coupling patterns originating from ^2H–^2H couplings are not visible on the 1D spectrum (generally included in linewidth), dipolar interactions between deuterium geminal exist and can participate to the signals. Here again, their contributions are not cumbersome for the analysis of spectra data, because whatever the manner, the aim of these sequences is to correlate the signal of non-equivalent geminal deuterium nuclei in oriented medium. Consequently, no modification of both 2D sequences was explored to remove them.

Finally, it was found experimentally an example of CD_2 system for which one of two deuterium–carbon total couplings is null. This rare case was observed at 300 K for solute **1** (50 mg) dissolved in an oriented solution of poly-ε-carbobenzyloxy-L-lysine (100 mg) and chloroform (350 mg). As expected by theory, the DECADENCY-INEPT 2D map (not reported here) shows exclusively diagonal and autocorrelation peaks associated with the deuterium nucleus coupled to the carbon atom.

4.1. Separation of NMR signals in a mixture

Encouraged by these results, we have investigated the case of a mixture of two dideuterated prochiral solutes. For our purpose we have prepared an equimolar mixture of **1** and 1-chloro[1-$^2H_2$]nonane (**2**) dissolved in the PBLG/$CHCl_3$ phase.

The ^2H–{^1H} 1D spectrum of the mixture is shown in Fig. 5A. The difference in intensity of pairs of doublets for **1** and **2** is a direct consequence of a significant ^2H–^2H homonuclear coupling for solute **1** that increases the linewidth, and so reduces the intensity of corresponding doublets. A gaussian filtering allows the measurement of the ^2H–^2H homonuclear coupling, i.e., 1.5 Hz. Figs. 5B and C present the DECADENCY-INEPT and DECADENCY-DEPT 2D maps obtained for the mixture. For both experiments, the delay τ is set to $1/(2T_{CD})$ while $\tau' = 1/(4T_{CD})$ and $\tau' = 1/(2T_{CD})$ were used for the INEPT-type and DEPT-type transfer, respectively. Considering the magnitude of ^2H–^{13}C total couplings for solute **1** (27 and 31 Hz), and **2** (around 34 Hz), the constant T_{CD} was kept to 29 Hz, which is close to the optimum value for the different deuterium nuclei.

As expected in both 2D experiments, the CP's are the dominant peaks on the 2D maps, and allow the correlation between the two pairs of quadrupolar doublets associated with geminal deuterium nuclei in solute **1** and **2**. However the dispersion of C–D couplings around T_{CD} prevents the total cancellation of peaks, which would be suppressed in the ideal case. As a result, residual peaks associated with DP's and AP's are more or less

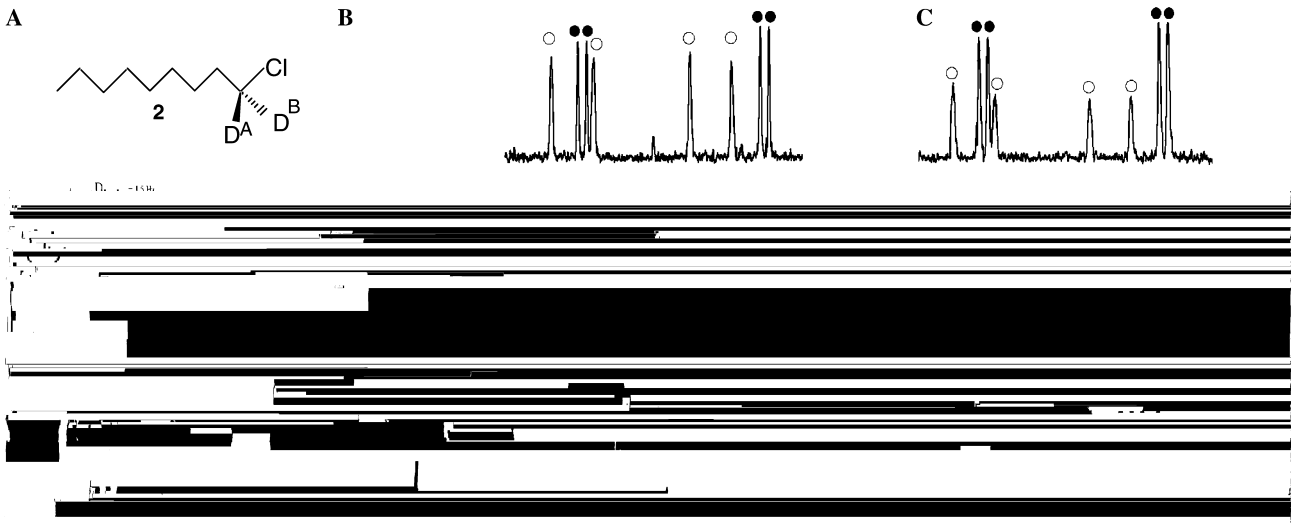

Fig. 5. (A) Structure of solute **2** and ^{2}H–{^{1}H} 1D spectrum of the mixture (**1** + **2**) in PBLG/$CHCl_3$ recorded with 64 scans and 2048 data points. In inset is shown the coupling pattern when a gaussian filtering (LB = −3 Hz, GB = 60%) is applied. (B) DECADENCY-INEPT 2D map of the mixture obtained when $\tau = 1/(2T_{CD})$, $\tau' = 1/(4T_{CD})$, with T_{CD} equals to 29 Hz. (C) DECADENCY-DEPT 2D map of the mixture obtained when $\tau = \tau' = 1/(2T_{CD})$. Both 2D spectra have been recorded using the same experimental conditions, using 128 (t_1) × 512 (t_2) data points and 320 scans per t_1. Filtering in both dimensions ($LB_{1,2} = 1$ Hz) and symmetrization were applied here. In F_1 dimension is displayed the 1D spectrum while in F_2 dimension is given the projection of the 2D map. Resonances marked by a star are associated with deuterated impurities. The quadrupolar splittings are equal to 193 and 361 Hz for solute **1** (labelled with open circles) and equal to 347 and 383 Hz for solute **2** (labelled with solid circles).

visible at lower level. Same reasons explain the presence of two pairs of CP's with low intensity perpendicular to the main diagonal in the case of DECADENCY-DEPT.

The position of the most intense CP's on the DECADENCY-DEPT 2D map indicates that the quadrupolar doublets have the same sign, positive or negative. To check this point we have recorded the ^{2}H–{^{1}H} 1D spectrum of the equimolar mixture of **1** and **2** dissolved in a racemic mixture of PBLG and PBDG (the enantiomer of PBLG) in chloroform. In such a solvent, noted hereafter PBG, spectral enantiodiscriminations are cancelled [19], and the quadrupolar splittings measured, $(\Delta\nu_Q)^{PBG}$, correspond to the algebraic average of splittings measured for D^A and D^B in the PBLG mesophase. In this example, the experimental values for solute **1** and **2** in PBG are equal to 292 and 368 Hz, while expected values would be equal to 277 and 365 Hz. As the compositions of the PBLG and PBG samples are identical, the observed discrepancies only reflect the difference of DP between PBLG (DP = 512) and PBDG (DP = 914, MW ≈ 200,000). This result proves that the signs of quadrupolar doublets are the same.

4.2. Phase sensitive experiment

As it is not possible to phase all resonances in pure absorption mode, the 2D maps of DECADENCY experiments are displayed in magnitude mode. The reason is that the signal is modulated by the quadrupolar splittings during the evolution τ delays (see in Eqs. (1) and (2)), thus leading to a phase modulation in F_1 and F_2 dimensions after the double Fourier transform.

The implementation of 90° pulses to refocus quadrupolar interaction during the fixed delays could be considered, but this solution generates several "irrelevant" terms in the density operators, thus leading to an important loss of sensitivity [20]. In the case of DECADENCY-INEPT 2D experiment, a possible alternative consists of simply removing the τ delays from the initial sequence and allowing the ^{13}C–^{2}H couplings to evolve during t_1 and t_2 periods. In practice, the ^{13}C π pulse in the midpoint of t_1 and the two τ intervals were removed while the deuterium decoupling is turned off during the acquisition. After a double Fourier transformation, a phased 2D map is expected with the same spectral information (δ_D, $^1T_{CD}$, and $\Delta\nu_Q$) in both dimensions. Note here that this solution is not applicable for the DECADENCY-DEPT 2D experiment because the signal evolves under the effect of the quadrupolar splittings during the $\tau'/2$ intervals as we can see in Eqs. (3)–(5).

To illustrate our purpose, we have recorded the phased DECADENCY-INEPT 2D experiment of **1** using $\tau' = 1/(4\ T)$ in order to maximize the intensity of CP's. As a result of the evolution of ^{13}C–^{2}H couplings during t_1 and t_2, 32 CP's (4 × 8) in pure absorption mode (16 positive peaks and 16 negatives) are now observed on the 2D spectrum shown in Fig. 6A. Actually the signals of quadrupolar doublets are in-phase while the two components resulting from the ^{13}C–^{2}H coupling are antiphase due to the absence of the delays τ. As a consequence of the non-equivalence of $^1T_{CD}$ for *pro-R* and *pro-S* deuteriums, the eight correlation sub-patterns between the two quadrupolar splittings do not form a square (see the inset). As previously residual DP's and

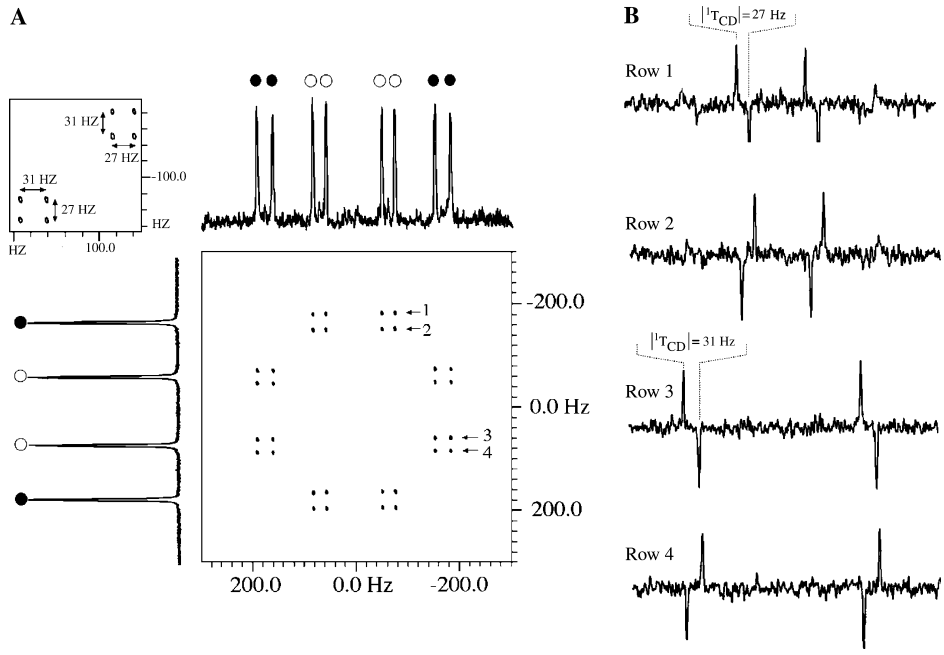

Fig. 6. (A) Phased variant of DECADENCY-INEPT 2D map of **1** obtained with no ^{13}C decoupling in F_2 and F_1 dimensions and using $\tau' = 1/(4T)$, with T_{CD} equal to 29 Hz. (B) Four rows extracted from the 2D map showing the phase of resonances. In inset is displayed a zoom of the 2D map. The 2D spectrum have been recorded using 128 (t_1) × 512 (t_2) data points and 320 scans per t_1. Filtering in both dimensions ($LB_{1,2} = 1$ Hz) was applied. In F_1 dimension is displayed the ^2H–{^1H} 1D spectrum of **1**, while in F_2 dimension is given the positive projection of the 2D map. The phase cycling of the phased DECADENCY-INEPT 2D experiment is identical to that of DECADENCY-INEPT 2D experiment. TPPI sampling scheme is used in F_1 dimension.

AP's are observed at very low level (not shown), however the 32 components (8×4) present a phase-twist lineshape. Calculations and computer simulations have confirmed this result.

Although possible, the application of the phased DECADENCY-INEPT experiments to analyse congested deuterium 1D spectra seems to be rather limited due to the substantial increase of peak numbers on the 2D map and the magnitude of the ^{13}C–^2H couplings.

5. Conclusion

We have theoretically and experimentally shown that it is possible to produce correlation between quadrupolar doublets of non-equivalent deuterium nuclei bonded to the same carbon in aligned solutes, using a double C–D polarization transfer of INEPT-type or DEPT-type. DECADENCY experiments exhibit no analytical complexity and under some conditions of timing ratio, the 2D maps are formally equivalent to ^2H–^2H COSY maps. In this work, the efficiency of these 2D experiments were illustrated using geminal deuteriums in prochiral molecules dissolved in a chiral liquid crystal. Obviously, these experiments could be successfully carried on for correlating any type of diastereotopic deuterium nuclei bonded to the same carbon atom, as in case of enantiomer solutes in chiral and non-chiral oriented solvents.

Acknowledgments

The authors thank Profs. J. Courtieu and B. Ancian for their helpful discussion.

Appendix A

To investigate theoretically the ^{13}C relayed ^2H–^2H-COSY 2D experiment, it is necessary to calculate analytically the time evolution of the density operator for a $^{13}CD_2$ group with two non-equivalent deuterium nuclei. For such spin system, there are 18 eigenvectors and the density operator is represented by a 18×18 dimension matrix. Assuming that the coupling between deuterium geminal nuclei are disregarded, analytical calculations can be greatly simplified by expressing the Hamiltonian and the density operator in a suitable orthogonal basis such as tensor operator product basis [21] or product operator basis [10,22]. We opted for the last one because it is more intuitive and provides much better physical insight. The 324 product operators for a $^{13}CD_2$ group are built from the product of the individual operators associated to a single carbon nucleus and two deuterons. For the carbon-13 nucleus, the usual Cartesian operators for spin-1/2, {E^C, S^C_x, S^C_y, and S^C_z} are retained [21]. For deuterium nuclei, the Cartesian operators for spin-1 recently reported were used [23]. This basis-set consists of the unit matrix E, the

angular moment operators for spin-1, I_x, I_y, and I_z, and five other operators denoted K_x, K_y, D_x, D_y, and Q_z.

The operators, K_x and K_y, defined as

$$K_x = I_xI_z + I_zI_x \text{ and } K_y = I_yI_z + I_zI_y, \quad (6)$$

represent the antiphase single-quantum magnetization of the quadrupolar doublet along the x and y axes, respectively. The operators, D_x and D_y, defined as

$$D_x = I_x^2 - I_y^2 \text{ and } D_y = I_xI_y + I_yI_x, \quad (7)$$

are the pure real and the pure imaginary spin-1 double quantum coherences. Finally, Q_z is the operator associated with the quadrupolar order and is equal to:

$$Q_z = 3I_z^2 - I^2. \quad (8)$$

This basis is advantageous because it provides a concise and relevant representation of Hamiltonians, coherences and polarization states in deuterium NMR spectroscopy in weakly oriented media. The rules describing the time evolution of individual spin-1/2 operators under radiofrequency pulses and chemical shifts are familiar [10,22]. The effect of radiofrequency

Table A
Evolution of product operators under the effect of heteronuclear IS coupling where $S = 1/2$ and $I = 1$

Coherence orders		$\hat{O}(0)$[a]	$\exp[-i(\omega t)2I_zS_z^C]\hat{O}(0)\exp[i(\omega t)2I_zS_z^C]$ with $\omega = \pi T$
p_S	p_I		
0	0	I_z	I_z
		Q_z	Q_z
		S_z^C	S_z^C
		$2I_zS_z^C$	$2I_zS_z^C$
		$2Q_zS_z^C$	$2Q_zS_z^C$
0	±1	I_x	$I_x\cos(\omega t) + 2I_yS_z^C\sin(\omega t)$
		I_y	$I_y\cos(\omega t) - 2I_xS_z^C\sin(\omega t)$
		K_x	$K_x\cos(\omega t) + 2K_yS_z^C\sin(\omega t)$
		K_y	$K_y\cos(\omega t) - 2K_xS_z^C\sin(\omega t)$
		$2I_xS_z^C$	$2I_xS_z^C\cos(\omega t) + I_y\sin(\omega t)$
		$2I_yS_z^C$	$2I_yS_z^C\cos(\omega t) - I_x\sin(\omega t)$
		$2K_xS_z^C$	$2K_xS_z^C\cos(\omega t) + K_y\sin(\omega t)$
		$2K_yS_z^C$	$2K_yS_z^C\cos(\omega t) - K_x\sin(\omega t)$
±1	0	S_x^C	$S_x^C\{2\cos(2\omega t)+1\}/3 + Q_zS_x^C\{\cos(2\omega t)-1\}/3 + I_zS_y^C\sin(2\omega t)$
		S_y^C	$S_y^C\{2\cos(2\omega t)+1\}/3 + Q_zS_y^C\{\cos(2\omega t)-1\}/3 - I_zS_x^C\sin(2\omega t)$
		$I_zS_x^C$	$I_zS_x^C\cos(2\omega t) + \{2S_y^C + Q_zS_y^C\}\sin(2\omega t)/3$
		$I_zS_y^C$	$I_zS_y^C\cos(2\omega t) - \{2S_x^C + Q_zS_x^C\}\sin(2\omega t)/3$
		$Q_zS_x^C$	$S_x^C\{2\cos(2\omega t)-2\}/3 + Q_zS_x^C\{\cos(2\omega t)+2\}/3 + I_zS_y^C\sin(2\omega t)$
		$Q_zS_y^C$	$S_y^C\{2\cos(2\omega t)-2\}/3 + Q_zS_y^C\{\cos(2\omega t)+2\}/3 - I_zS_x^C\sin(2\omega t)$
±1	±1	$I_xS_x^C$	$I_xS_x^C\cos(\omega t) + K_xS_y^C\sin(\omega t)$
		$I_xS_y^C$	$I_xS_y^C\cos(\omega t) - K_xS_x^C\sin(\omega t)$
		$I_yS_x^C$	$I_yS_x^C\cos(\omega t) + K_yS_y^C\sin(\omega t)$
		$I_yS_y^C$	$I_yS_y^C\cos(\omega t) - K_yS_x^C\sin(\omega t)$
		$K_xS_x^C$	$K_xS_x^C\cos(\omega t) + I_xS_y^C\sin(\omega t)$
		$K_xS_y^C$	$K_xS_y^C\cos(\omega t) - I_xS_x^C\sin(\omega t)$
		$K_yS_x^C$	$K_yS_x^C\cos(\omega t) + I_yS_y^C\sin(\omega t)$
		$K_yS_y^C$	$K_yS_y^C\cos(\omega t) - I_yS_x^C\sin(\omega t)$
0	±2	D_x	$D_x\cos(2\omega t) + 2D_yS_x^C\sin(2\omega t)$
		D_y	$D_y\cos(2\omega t) - 2D_xS_z^C\sin(2\omega t)$
		$2D_xS_z^C$	$2D_xS_z^C\cos(2\omega t) + D_y\sin(2\omega t)$
		$2D_yS_z^C$	$2D_yS_z^C\cos(2\omega t) - D_x\sin(2\omega t)$
±1	±2	$D_xS_x^C$	$D_xS_x^C$
		$D_xS_y^C$	$D_xS_y^C$
		$D_yS_x^C$	$D_yS_x^C$
		$D_yS_y^C$	$D_yS_y^C$

[a] The identity operators for $I = 1/2$ and $S = 1$ are omitted. $\hat{O}(0)$ corresponds to the initial operator at time $t = 0$.

pulses, chemical shifts, and quadrupolar couplings on the spin-1 operators were reported in [23]. In contrast, if some evolution rules of product operators or tensor product operators under coupling between spin-1 and spin-1/2 have been reported previously [10,22,24,25], they are not exhaustive.

To the best of our knowledge, the evolution of the antiphase single-quantum magnetizations of the quadrupolar doublet and those of the spin-1 double quantum coherences under the coupling have never been presented so far. To investigate thoroughly ^{13}C relayed ^{2}H–^{2}H-COSY 2D experiment, we have to conveniently determine the rules describing the evolution of the 36 relevant product operators corresponding to an IS system, where $S = 1/2$ and $I = 1$, under the effect of heteronuclear coupling Hamiltonian. For our purpose, we used the basis-sets mentioned above and the algebraic density matrix calculations were computed using the software *Mathematica* [15]. The explicit results are presented in Table A.

References

[1] I. Canet, J. Courtieu, A. Loewenstein, A. Meddour, J.-M. Péchiné, Enantiomeric analysis in a polypeptide lyotropic liquid crystal by deuterium NMR, J. Am. Chem. Soc. 117 (1995) 6520–6526.

[2] P. Lesot, M. Sarfati, J. Courtieu, Natural abundance deuterium NMR spectroscopy in polypeptide liquid crystals as a new and incisive means for enantiodifferentiation of chiral hydrocarbons, Chem. Eur. J. 9 (2003) 1724–1745.

[3] M. Sarfati, P. Lesot, D. Merlet, J. Courtieu, Theoretical and experimental aspects of enantiomeric differentiation using natural abundance multinuclear NMR spectroscopy in polypeptide liquid crystals, Chem. Commun. (2000) 2069–2081, and references therein.

[4] C. Aroulanda, M. Sarfati, J. Courtieu, P. Lesot, Investigation of enantioselectivity of three polypeptide liquid-crystalline solvents using NMR spectroscopy, Enantiomer 6 (2001) 281–287.

[5] H. Villar, F. Guibe, C. Aroulanda, P. Lesot, Investigation of SmI_2 mediated cyclisation process of δ-iodo-α, β-unsaturated esters by deuterium 2D NMR in oriented solvents, Tetrahedron: Asymmetry 13 (2002) 1465–1475.

[6] P. Lesot, M. Sarfati, D. Merlet, B. Ancian, J.W. Emsley, B.A. Timimi, 2D-NMR strategy dedicated to the analysis of perdeuterated enantiomer solutes in weakly ordered chiral liquid crystals, J. Am. Chem. Soc. 125 (2003) 7689–7695.

[7] O. Lafon, P. Berdagué, P. Lesot, Use of two-dimensional correlation between ^{2}H quadrupolar splittings and ^{13}C CSA's for assignment of NMR spectra in chiral nematics, Phys. Chem. Chem. Phys. 6 (2004) 1080–1084.

[8] M.A. Delsuc, E. Guittet, N. Trotin, J.-Y. Lallemand, Two-dimensional correlation spectroscopy with heteronuclear relay, J. Magn. Reson. 56 (1984) 163–166.

[9] D. Neuhaus, G. Wider, K. Wagner, K. Wüthrich, X-relayed ^{1}H–^{1}H correlated spectroscopy, J. Magn. Reson. 57 (1984) 164–168.

[10] R.R. Ernst, G. Bodenhausen, A. Wokaun, Principles of Nuclear Magnetic Resonance in One and Two Dimensions, Clarendon Press, Oxford, 1987.

[11] G.A. Morris, R. Freeman, Enhancement of nuclear magnetic resonances signals by polarization transfer, J. Am. Chem. Soc. 101 (1979) 760–762.

[12] D.M. Doddrell, D.T. Pegg, M.R. Bendall, Distortionless enhancement of NMR signals by polarization transfer, J. Magn. Reson. 48 (1982) 323–327.

[13] J. Shriver, NMR product-operator calculations in mathematica, J. Magn. Reson. 94 (1991) 612–616.

[14] P. Güntert, N. Schaeffer, G. Otting, K. Wüthrich, POMA: a complete mathematica implementation of the NMR product-operator formalism, J. Magn. Reson. Ser. A 101 (1993) 103–105.

[15] Wolfram Inc., Mathematica, Version 4.2, Champaign, IL, 2002.

[16] J. Keller, R.T. Clowes, A.L. Daies, E.D. Laue, Pulsed-field gradients: theory and practice, Methods Enzymol. 239 (1994) 145–207.

[17] T.T. Nakashima, R.E.D. McClung, B.K. John, Experimental and theoretical investigation of ^{2}D–^{13}C DEPT spectra on CD_n systems, J. Magn. Reson. 58 (1984) 27–36.

[18] C. Aroulanda, D. Merlet, J. Courtieu, P. Lesot, NMR experimental evidence of the differentiation of enantiotopic directions in C_s and C_{2v} molecules using partially oriented, chiral media, J. Am. Chem. Soc. 123 (2001) 12059–12066.

[19] C. Canlet, D. Merlet, P. Lesot, A. Meddour, A. Loewenstein, J. Courtieu, Deuterium NMR Stereochemical Analysis of *threo-erythro* isomers bearing remote chiral centres in racemic and non-racemic liquid crystalline solvents, Tetrahedron: Asymmetry 11 (2000) 1911–1918.

[20] S. Antonijevic, S. Wimperis, Refocussing of chemical and parametric shift anisotropies in ^{2}H NMR using the quadrupolar–echo experiment, J. Magn. Reson. 164 (2003) 343–350.

[21] N. Müller, G. Bodenhausen, R.R. Ernst, Relaxation-induced violation of coherence transfer selection rules in nuclear magnetic resonance, J. Magn. Reson. 75 (1987) 297–334.

[22] O.W. Sorensen, G.W. Eich, M.H. Levitt, G. Bodenhausen, R.R. Ernst, Relaxation-induced violation of coherence transfer selection rules in nuclear magnetic resonance, Prog. NMR Spectrosc. 16 (1983) 163–192.

[23] D. Merlet, M. Sarfati, B. Ancian, J. Courtieu, P. Lesot, 2D-NMR strategy dedicated to the analysis of perdeuterated enantiomer solutes in weakly ordered chiral liquid crystals, Phys. Chem. Chem. Phys. 2 (2000) 2283–2290.

[24] N. Chandrakumar, Polarization transfer between spin-1 and spin-1/2 Nuclei, J. Magn. Reson. 60 (1984) 28–36.

[25] R. Kemp-Harper, D.J. Philip, P.W. Kuchel, Nuclear magnetic resonance of *J*-coupled quadrupolar nuclei: use of the tensor operator product basis, J. Chem. Phys. 115 (2001) 2908–2916.